2007

Crystallographic analysis of Parasponia andersonii hemoglobin

Andrea Savage
Iowa State University

Crystallographic analysis of *Parasponia andersonii* hemoglobin

by

Andrea Savage

A thesis submitted to the graduate faculty

in partial fulfillment of the requirements for the degree of

MASTER OF SCIENCE

Major: Biochemistry

Program of Study Committee:
Mark Hargrove, Major Professor
Alan Dispirito
Xueyu Song

Iowa State University

Ames, Iowa

2007

TABLE OF CONTENTS

LIST OF FIGURES

LIST OF TABLES

ABSTRACT

The x-ray crystal structure of ferric *Parasponia andersonii* hemoglobin has been determined to 2.3 Å resolution by molecular replacement with Rice hemoglobin 1 (rHb1). By means of absorbance spectroscopy, electrochemistry and x-ray crystallography, it has been revealed that depending on the oxidation state, the heme iron can exsist in either the pentacoordinate or hexacoordinate form. Pentacoordination of the heme iron is found primarily in the deoxy ferrous (2+) form, whereas the ferric (3+) form is exhibited predominantly in bis-histidine coordination. This is unique among known forms of hemoglobins. Furthermore, the crystallographic data has provided evidence which supports previous works reporting hexacoordination of the heme iron more closely associated with the ferric state (11).

CHAPTER 1: INTRODUCTION

Background

Hemoglobins play a large role in many physiological functions of great importance. Most are familiar with hemoglobin found in red blood cells, myoglobin found in the muscles, or leghemoglobin in the root nodules of soybeans, all of which facilitate the transport of oxygen.

In more recent years, a new class of Hbs has been identified in plants termed non-symbiotic hemoglobins (nsHbs) (6). The first nsHb gene was identified in non-nodulating *Trema tomentosa* based on its relation to *Parasponia andersonii*, a nodulating non-legumous plant (2). Since, homologous Hbs have been identified in many other species and are now believed to be found in most organisms including humans. Some examples of hxhbs in humans are neuroglobin (Ngb), expressed in the brain and cytoglobin (Cgb) which is found throughout the body (14). Although the absolute function of these proteins has yet to be fully determined, their levels of expression and oxygen dissociation rates are too low to be physiologically relevant as oxygen transporters (3). However, nsHbs have been associated with plant disease response, germination, somatic embryogenesis and hypoxia to name a few (1).

The distinguishing characteristic between these newly discovered Hbs and previously known Hbs, is coordination of an additional histidine to the the distal side to the heme iron at the

sixth position, similar to cytochrome *b5,* a electron transport hemeprotein. Thus arose the term hexacoordinate hemoglobin (hxHb). Interestingly, cytochrome *b5* is unreactive toward diatomic ligands, whereas hxHbs are able to bind oxygen, other gaseous ligands and small molecules with high affinities (5).

Hemoglobins

In plants, there are at least three distinct types of hemoglobins: symbiotic, nonsymbiotic, and truncated hemoglobins. All plant hemoglobins found so far, are either monomers or homodimers.

Hbs are characterized by a globin fold of six to eight helicies named A though H. The globin fold contains heme as a prosthetic group (3). The helices within the globin fold are organized into a two-layer structure, known as a three-on-three alpha helical sandwich. In the case of truncated hemoglobins, which are 20-40 amino acids shorter than other globins, a two-on-two sandwich of alpha helices (13).

Heme consists of a porphyrin ring structure with a central iron atom. A porphyrin ring is made up of four pyrrole rings linked by methene bridges. The iron can exist either in its ferrous, reduced Fe^{2+} form or in its ferric oxidized Fe^{3+} form. This structure is key during

electron transfer, redox reactions, ligand transport, or enzymatic catalysis (7). Also the characteristic red color of Hbs can be attributed to heme.

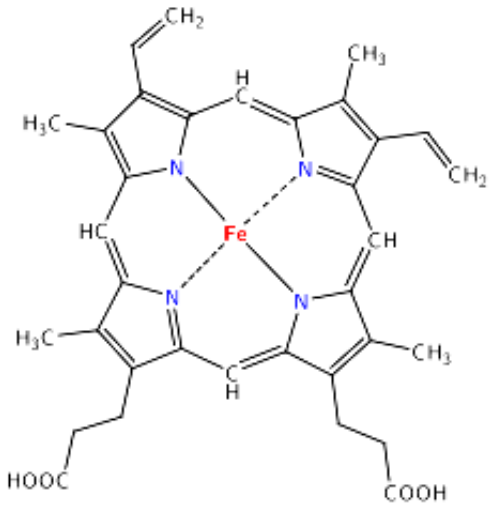

Fig. 1 Heme B found in Hb and myoglobin

Hbs can be generally classed as either pentacoordinate or hexacoordinate. Pentacoordinate meaning the heme iron is coordinated at five of the six available sites. The heme iron is coordinated to four nitrogens and a histidine on the proximal side. The sixth site is uncoordinated and is where ligands interact (14). Ligand binding is regulated by the heme iron and both steric and electrostatic configuration of the distal heme pocket. Hemoglobin and myoglobin are examples of pentacoordinate Hbs. Typically, in the unliganded or deoxy state, Hbs are pentacoordinate and when oxidized, coordinate a water (4).

On the other hand, hxHbs are hexacoordinate in the absence of exogenous ligands. The heme iron is coordinated at all six positions. Hexacoordination is influenced by amino acids lying in the vicinity of the heme pocket and their interactions with the distal histidine (11). Ligand binding is regulated through the coordination of an amino acid side chain to the ligand binding site of the heme iron. The reversible coordination of the heme iron by the distal histidine makes ligand binding very complex. Still though, relative to pentacoordinate Hbs, they are still able to bind ligands with very high affinity (6). Kinetic data has helped in

understanding the mechanisms of their activity and outlined plausible functions but their true functions still remain a mystery.

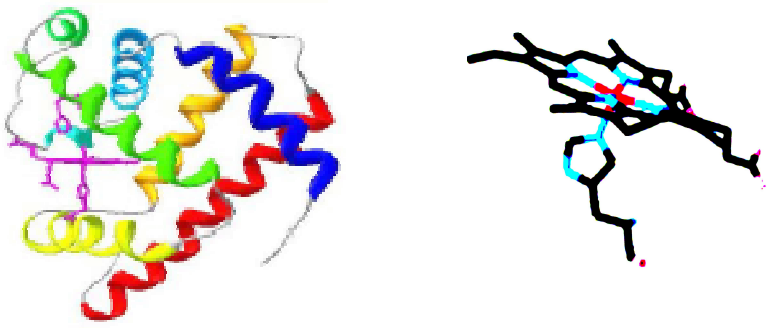

Fig.2 An example of pentacoordination

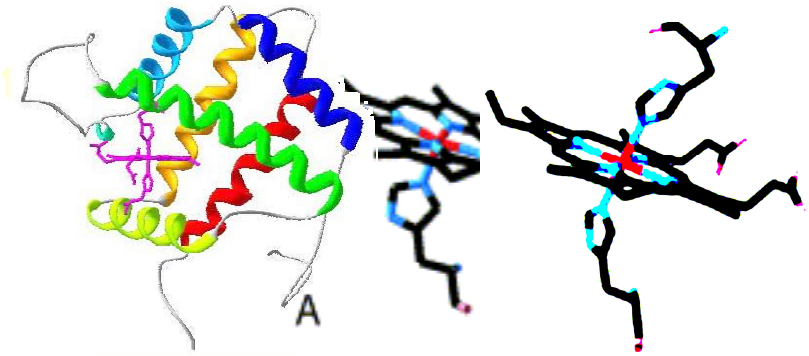

Fig. 3 An example of hexacoordination

Pentacoordinate and hexacoordinate hemoglobins can be distinguished according to their absorbance spectra. For a pentacoordinate heme in the ferrous form, there is a single broad absorbance band at roughly 550 nm (fig. 5). In hexacoordination, that single broad band is split into two separate peaks around 550 nm (fig. 6) . The difference in the absorbance spectrum between the two forms is largely attributed to the spin state due to the electrostatic

field around the heme. High/low spin states are a result of two unpaired/paired electrons of the uppermost orbital. A high spin state is reminiscent of pentacoordination, where as a low spin state is associated with hexacoordination (9).

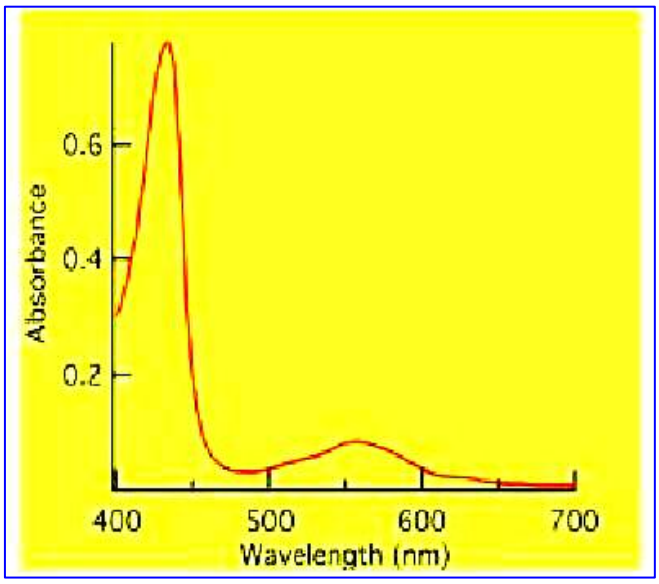

Fig. 4 Example of ferrous pentacoordinate hemoglobin absorbance spectrum in the visible region

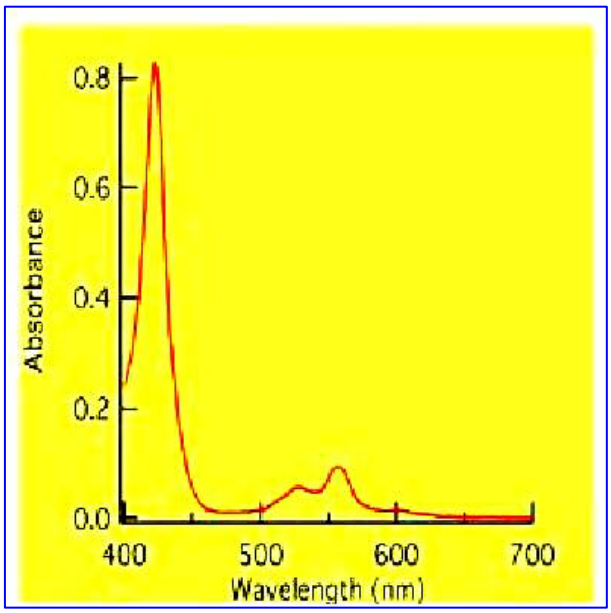

Fig. 5 Example of ferrous hexacoordinate hemoglobin absorbance spectrum in the visible region

At first glance, spectral differences are quite obvious in the ferrous state and both forms are easily distinguishable. Although not quite as pronounced, both forms can also be distinguished in their ferric states. This will be discussed later.

Parasponia andersonii

Parasponia andersonii is a medium size (up to 20 m) tropical tree belonging to the *Ulmacea* (Elm) tree family. It is native to the Malay Archipelago, which is comprised of roughly twenty thousand islands laying between mainland southeastern Asia and Australia.

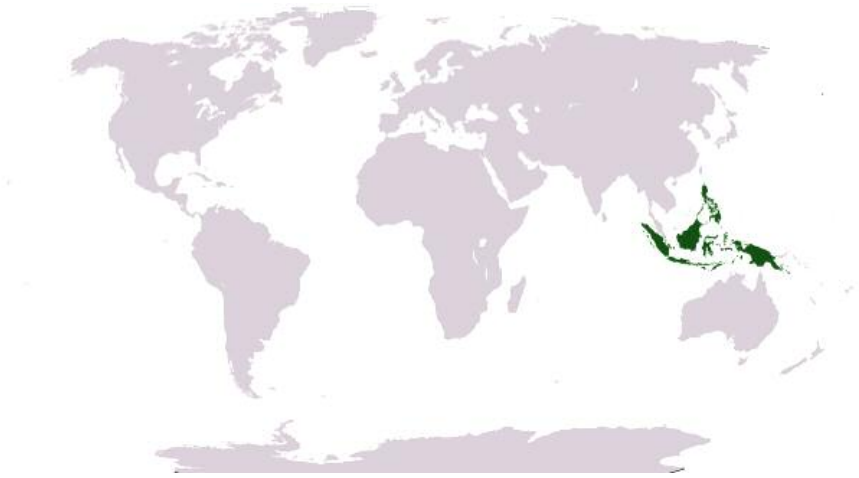

Fig. 6 Location of Malay Archipelago highlighted in dark green

Plant Hbs were first discovered in the root nodules of soybeans, where it exsist in a symbiotic relationship with rhizobia. It is generally accepted that their role is to facilitate oxygen diffusion to the rhizobia. For a long time Hbs in plants were only associated with legumes. In 1983, work was published identifying Hb in the nitrogen-fixing root nodules of *Parasponia*

andersonii, a non-legume dicot. Parasponia is the only known non-legume associated with nitrogen-fixing and rhizobia (12, 15).

The hemoglobin gene in Parasponia is expressed in both nodules and non-nodulated roots, suggesting that Parasponia Hb may have symbiotic and nonsymbiotic roles (12). Upon examination of the amino acid sequence, Parasponia most closely identifies with the nsHb group yet kinetically it has characteristics of symbiotic Hbs (2).

Justification

Parasponia hemoglobin absorption spectra of deoxy-ferrous, O_2- ferrous, and CO- ferrous as well as kinetic constants are similar to that of pentacoordinate Leghemoglobins (Lbs). It is thought to maintain a similar role to Lbs in facilitating the diffusion of oxygen (15). However, interestingly, in observing absorbance spectra, depending on the oxidation state of the heme iron, Parasponia appears to be either pentacoordinate in the ferrous (2+) or hexacoordinate in the ferric (3+) state.

Approach

Absorption Spectroscopy

Pentacoordinate and hexacoordinate hemoglobins can be distinguished according to their absorbance spectra in the visible region. For a pentacoordinate heme in the ferrous form, there is a single broad absorbance band at roughly 550 nm (fig. 5). In hexacoordination, that single broad band is split into two separate peaks around 550 nm (fig. 6). The difference in

the absorbance spectrum between the two forms is largely attributed to the spin state due to the electrostatic field around the heme. High/low spin states are a result of two unpaired/paired electrons of the uppermost orbital. A high spin state is reminiscent of pentacoordination, where as a low spin state is associated with hexacoordination.

Electrochemistry

The free energy needed to reduce a Hb from the ferric to the ferrous form is measured by the midpoint potential. Midpoint potentials for pentacoordinate Hbs tend to be positive whereas hxHbs are negative with respect to a standard hydrogen electrode (SHE). For example, myoglobin has a midpoint potential of +60 mV in comparison to rHb1 at -143 mV. Meaning, thermodynamically, in the reduced form pentacoodinate Hbs are more stable than hxHbs. A more negative midpoint potential (relative to a pentacoordinate Hb) also implys tigher hexacoordination in the ferric state as to ferrous.

X-ray Crystallography

X-ray crystallography is a technique which allows the visualization of protein structure near the atomic level. There are three basic steps to protein x-ray crystallography. First, the protein is crystallized. Second, the crystal is placed in a beam of x-rays at a single wavelength producing reflections of certain intensities at many angles. Lastly, with the aide of computer software, a model of the protein‘s arrangement in the crystal is produced from the data provided. The reflections and electron density are related by the mathematical operation called a Fourier transform (equ. 1).

$$F(\boldsymbol{h}) = \int_{unitcell} f(\boldsymbol{x}) \exp(i\boldsymbol{x}\cdot\boldsymbol{h})\, dx$$

Equ. 1 F(h) is a vector containing the amplitude and the phase of the reflection, which is the reflection at reciprocal lattice point h. F(x) is the scattering function of the electron density at point x.

Phase problem

There are two parts needed to calculate electron density, intensity and phase but only intensity can be measured. Thus, the phases must be derived by other means such as multiple isomorphous replacement, molecular replacement or multiple wavelength anomalous dispersion (MAD). With Multiple Isomorphous Replacement, heavy atoms are soaked into the crystal and several data sets are collected. For Multiple Wavelength Anomalous Dispersion (MAD), Diffraction is measured at several different wavelengths near the absorption edge of a heavy-atom. Lastly, in molecular replacement, homologous structure (with known phases) and the diffraction data for the unknown structure are superimposed.

Refinement

There are several ways in which the quality of a model can be evaluated. One principle way is by monitoring the R-factor, which is defined as the agreement between a model and the original x-ray diffraction data (equ. 2).

$$R = \frac{\sum ||F_{obs}| - |F_{calc}||}{\sum |F_{obs}|}$$

Equ. 2 Definition of R-factor (R). F_{obs} is the measured intensity of reflection in diffraction pattern. F_{calc} is intensity of the same reflection calculated in the current model.

An R-factor equal to zero would mean perfect agreement. A value less than 0.5 says more data is needed and above 0.5 meaning the agreement between the observed and calculated intensities are very poor. Stillthough, even models with a low R value could be subjected to over refinement. Hence, R_{free} is used in cross validation. R_{free} is caluculated in the same way as R but instead a set of randomly choosen intensities are set aside from the beginning and not used during refinement. In this way it measures how well the current model predicts the set of measured reflection intensities not included in refinement. Whereas R measures how the current model predicts the enitre data set. In the intermediate stages of refinement R_{free} is larger than R, but in the final stages the two become more similar (10).

CHAPTER 2: RESULTS

Absorption Spectroscopy

The ferrous form of parasponia hemoglobin, reveals a Soret peak at 424 nm and a broad band at 556 nm (Fig. 9). This is characteristic of a pentacoordinated heme with the iron in the high spin state. To the contray, the typical absorption for ferrous hexacoordinate globins is a soret peak at 424 nm and then two separate peaks around 550 nm as in the case with rHb1 (see figure 5).

In the ferric form the Soret shifts to 408 nm with a broad peak at 531 nm (fig. 2). The shape of the shoulder of the peak is an earmark of a hexacoordinated heme, iron in the low spin state. Similar values were reported for rHb1 (4). Whereas, the typical absorbance maxima for ferric pentacoordinate globins is a soret peak around 408, and a relatively undefined peak between 500 and 600 nm. Its easiest to distinguish between both pentacoordinate and hexacoordinate forms by comparing spectra in the visible region side by side. As seen in figure 10 there is a particular shape to the shoulder of the soret curve, making it easy to discriminate between the two forms. The purple and green lines are represented by hxHbs, cytogobin and rHb1, respectively. The orange and blue lines, pentacoordinate proteins, horse heart myoglobin and lupin. Parasponia is in red and and appears most similar to rHb1 and cytoglobin.

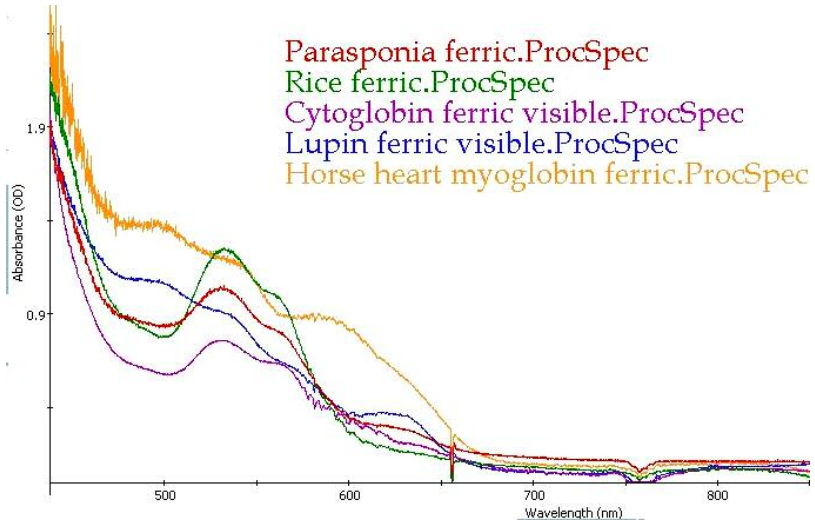

Fig. 7 Overlay of rhb1, Cyt, Lupin, and horse heart myoglobin illustating the hexacoordinate character of parasponia.

Electrochemistry

The change in the absorption was measured at 424 nm and the corresponding cell potential was noted after each addition of dithionite solution. The midpoint potential, -135 mV was determined from Equation 3. The negative midpoint potential indicates that hexacoordination in parasponia is tighter in the ferric versus the ferrous state (11).

$$F_{\text{reduced}} = \frac{e^{-\left(\frac{nF(E_{\text{obs}} - E_{\text{mid}})}{RT}\right)}}{1 + e^{-\left(\frac{nF(E_{\text{obs}} - E_{\text{mid}})}{RT}\right)}}$$

Eq. 3 The fraction of protein reduced, F_{educed} is the normalized change in absorbance at 424 nm, E_{obs} the observed cell potential, and E_{mid} the midpoint potential obtained by fitting the experimental data to Eq. 3 (5).

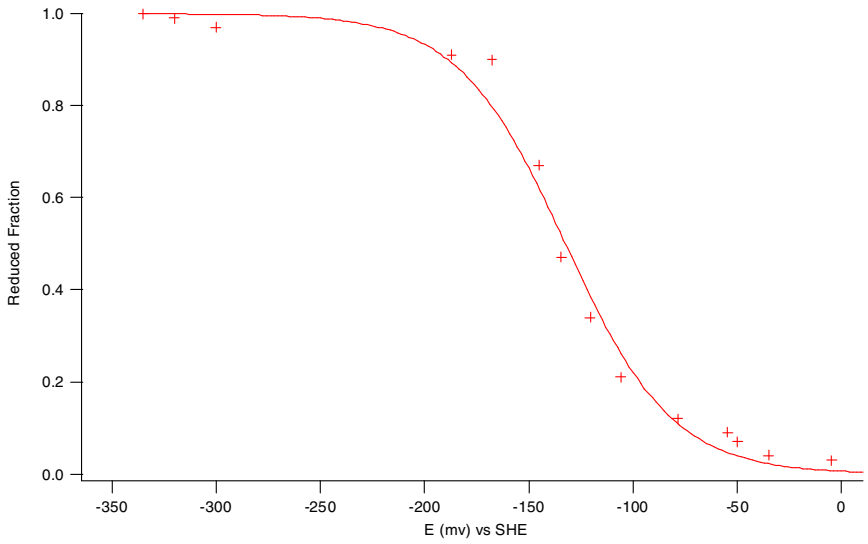

Fig. 8 Dithionite titration of Parasponia Hb

TABLE 1. Midpoint potentials of various Hbs (5,11)

Protein	Coordination	Midpoint potential (mV)
Rice	hexa	-143
Cytoglobin	hexa	-28
Neuroglobin	hexa	-115
Myoglobin	penta	+60
Leghemoglobin	penta	+20

Midpoint potentials for pentacoordinate Hbs tend to be positive whereas hxHbs are negative with respect to a standard hydrogen electrode (SHE). For example, myoglobin has a midpoint potential of +60 mV in comparison to rHb1 at -143 mV. Meaning, thermodynamically, in the reduced form pentacoodinate Hbs are more stable than hxHbs. A

large drop in redoxpotential suggests the possibility of tighter hexacoordination in the ferric as to the ferrous state (11).

X-ray Crystallography

Parasponia crystallized in orthorombic space group P212121.

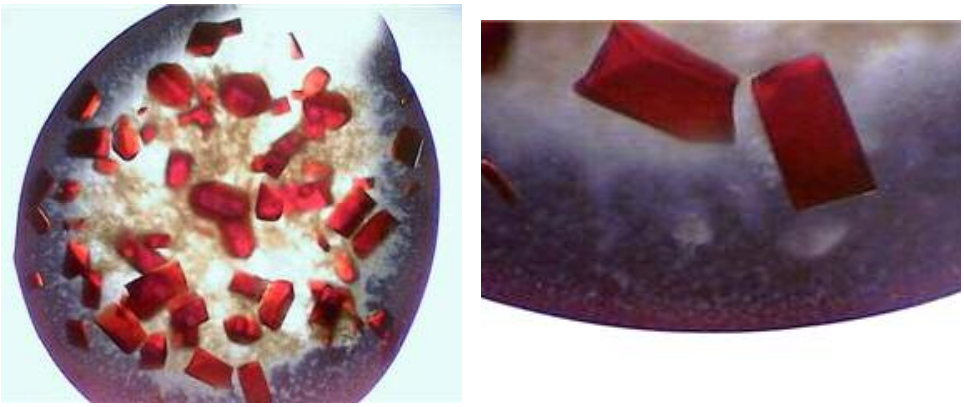

Fig.9 Parasponia Hb crystals

Table 1. Data collection and refinement statistics

Residues	324
Protein atoms	2491
A. Crystal data	
Space group	P212121
a, b, c (Å)	55.04, 72.04, 88.32
B. Data processing	
Resolution range (Å)	37.65-2.3 (2.38-2.3)

Total reflections	109558
Unique reflections	16210
Completeness (%)	100% (100%)
R_{merge}	0.154 (0.641)
Average I/ σ I	10.7 (4.2)
Mosaicity	2.142

C. Refinement

$R_{crystal}$	0.22
R_{free}	0.26
rms values	
Bond lenghts (Å)	0.038
Bond angles (°)	3.241
Water molecules	184

Ramachandran plot (%)

Preferred	91.3
Allowed	7.2
Generously allowed	1.1
Disallowed	0.4

The numbers in parentheses are the outer-shell statistics, 2.36- 2.3 Å.

Throughout refinement, Rfree (calculated from 5.4% of the data) was used to monitor progress. The final model contains water 184 molecules, has an R factor 0.22 R_{free} of 0.26. 99.6% of the backbone conformations are in the allowed regions of the Ramachandran plot

(Table 1). The final model was selected according to the best improvement in the R-factor.

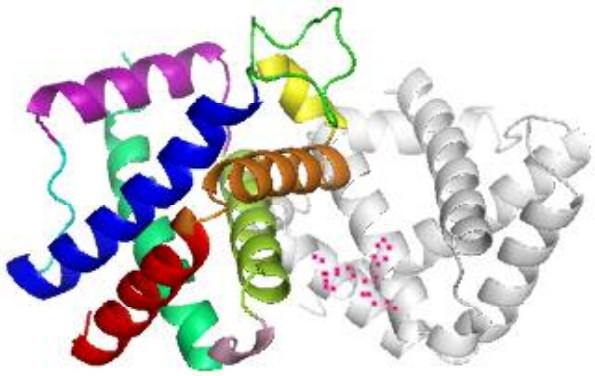

Fig. 10 Parasponia Hb. A helix/N terminus (Red), B helix (Orange), C helix (Yellow), CD loop (Green), D helix (Blue), DE loop (Cyan), E helix (Purple), F helix (Olive green), G helix (Pink), H helix/C terminus (Turquoise).

The model shows that the protein is a homodimer, each subunit (A, B) 162-residues in length. Each subunit contains a heme b prosthetic group with bonds between the heme iron and the distal (His 70) and proximal (His 105) histidines (Figure 1). The molecular weight of a subunit is 18,795 Da or 18,178 Da without heme. The tertiary structure consists of seven helices that correspond to the A, B, C, D E, F, and H helices.

In calculating R and R_{free} several regions of amino acids were left out either because there was no or poor density. These regions correspond to the termini and select loop regions which are unrestrained in movement relavtive to the ordered arrangement of α helices. Therefore, calculating well defined electon density can be difficult. The following residues were omited in Chain A; 1-8, 54-61, and 158-162 corresponding to the N teminus, CD loop, C terminus regions, respectively. In Chain B the following residues were omited: 1-9 and

160-162 corresponding to the N teminus and C teminus, respectively. Although there was density for residues 50-67 in the CD loop region of the B chain, the area was quite disordered. As seen in the ramachandran plot, residues in the generously and disallowed regions are part of Chain B's CD region, with the exception of Met 158 (chain B) which is located in the C terminal region. Despite those few disordered regions the backbone seems pretty good. More than 99% of the torsional angles are in the allowed regions of a Ramachandran plot (Table 2).

The heme pocket of parasponia has the distal histidine His70 (E7) coordinating to the heme iron atom. The heme pocket also contains all known conserved residues among Hbs, namely Phe36 (B10), Phe51 (CD1) and Val 74 (E11) (7, fig. 13).

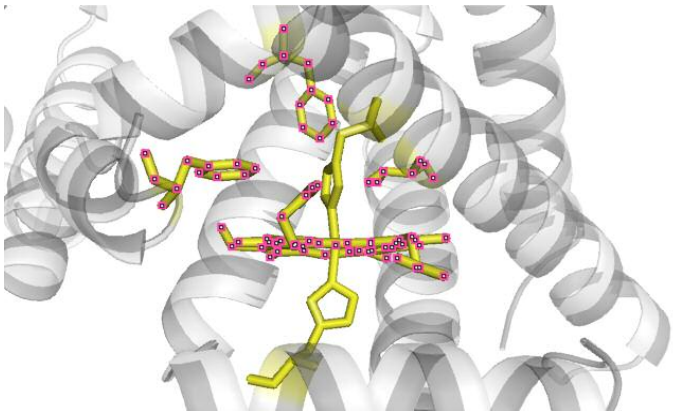

Fig. 11. Key residues in the heme pocket of parasponia Hb. In clockwise order starting at noon: PheB10, HisE7, ValE11, HisF8, PheCD1

Parasponia shares a sequence idenity of 37.7% with Lba and 64.1% with rHb1. Many models were tested but rHb1 (PDB code 1DU8) proved to be the best fit as a molecular replacement

model with an initial crystallographic R_{free} of ~0.45 indicating the two molecules did share some similarites. However, upon refinenment of the parasponia model it resembled rHb1 almost identically (fig 12). The resolution of rHb1 was 2.35 Å and parasponia 2.3 Å, meaning minor differences their structures may not be apparent.

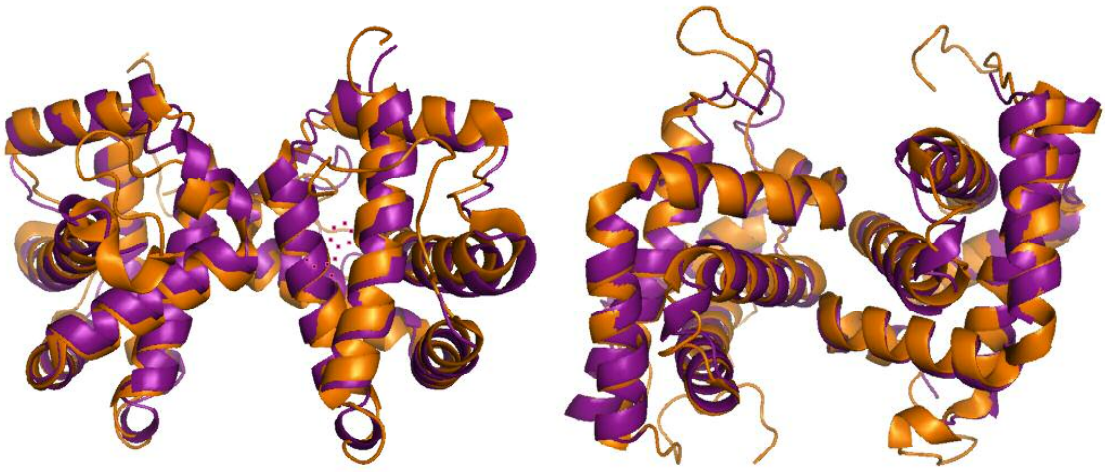

Fig. 12 RHb1 in orange and parasponia in purple. Parasponia contains 162 residues, 4 less than rHb1.

Through the years, several residues in the heme pocket have been identified to be important in ligand binding. These are B10, CD1, and E11. The heme pocket of parasponia is very similar to rHb1. Both have in common Phe36 (B10), Phe51 (CD1) and Val 74 (E11). One difference was G8 which in rHb1 is a leucine but in parasponia an isoleucine. Areas which make up the dimer interface are the B helix, CD loop, and G helix. The residues which create the dimer interface in parasponia are also found in rHb1 as well as other plant Hbs (7).

Interestingly, the proposed model shares more identity with rHb1 (fig. 13) than Lba (fig.14).

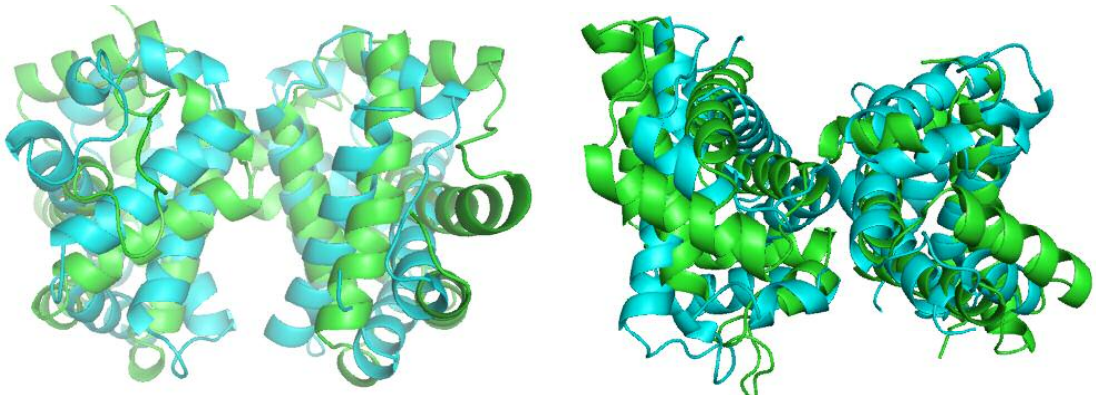

Fig. 13 Parasponia in green and Lba in blue. Parasponia contains 162 residues, 20 more than Lba.

One difference is Parasponia hemoglobin is dimeric whereas Lba is monomeric. In figure 14 it is aligned with both of parasponia's subunits to illustrate their structural differences at several angles. In Lba, key residues of the interface in parasponia are replaced by nonhydrophobic amino acids, which prevent dimer formation by disrupting the hydrophobic core. In the heme pocket the most noticable difference is the position of the distal histidine in relation to the heme iron. The distance is much greater in Lba than in parapsonia. The distal histidine is actaully coordinated to the heme iron where as in Lba it is not. Other difference in residues include Tyr B10 and Leu Ell as opposed to Phe and Val in parasponia.

The do share the same residue for CD1, phenylalanine.

CHAPTER 3: DISSCUSION

Parasponia Hb is thought to maintain the same role as pentacoordinate Lba because of similar kinetic constants and expression in root nodules (15). As seen in the structural analysis, parasponia more closely resembles rHb1. In fact, the structures resemble each other very much from the positions of the helices to key residues found in the heme pocket as discussed earlier. I was unable to find differences of huge significance.

This could be related in part to the resolution of the structure. The resolution of rHb1 was 2.35 Å and for parasponia 2.3 Å. The resolutions here are such that minor structural changes may go unnoticed. In any case a higher resolution data set of parasponia should be recollect for a more refined structure.

However, in comparison to Lba, parasponia proved to be quite different, even in the heme pocket. The distal histidine is actaully coordinated to the heme iron in parasponia where as in Lba it is not. Other difference in residues include Tyr B10 and Leu Ell as opposed to Phe and Val in parasponia.

The midpoint potential of parasponia was -135 mV. This potential is also very close to rHb1's, -143 mV. Meaning, thermodynamically, in the reduced form pentacoodinate Hbs are more stable than hxHbs. A more negative midpoint potential (relative to a pentacoordinate Hb) also implys tigher hexacoordination in the ferric state as to ferrous (11). This is supported by the model in which ferric parasponia Hb is found to be hexacoordinate.

Analysis of parasponia's absorbance spectra shows pentacoordinate characteristics in the ferrous state. Hbs only bind ligands such as O_2 and CO in the ferrous state. Perhaps in the reduced state large conformational changes take place rendering a structure that shares less identity with rHb1 and more with Lba. For futrue studies it would be very interesting to be able to compare structures of both the reduced and oxidized forms of the protein. Also ligands such as CN^- and N_3 are able to bind the heme iron in the ferric form. It would be interesting to compare the results with other known hexacoordinate proteins. And then to relate the different functional properties of parasponia with its structural properties. But then again there could be other factors that influence heme coordination such as pH. These should be further investigated too. All in all parasponia is an excellent model of a hemoglobin which exhibits behavior of the well-defined pentacoordinate Hbs, yet structurally similar to hxHbs of unknown function.

CHAPTER 4: METHODS

Parasponia Hb Expression

Cyril Appleby from Australia kindly provided plasmid. Protein was over-expressed in Novagen Rosettablue cells (DE3). Cells grew in twelve, one-liter flasks of 2XYT media and 500 μL of antifoam (Sigma) with 2 g/L of Lactose. Isopropyl-1-thio-β-D- galactopyranoside and free hemin was not added during fermentation. For selection 50 μg/ml of both kanamyacin sulfate and chloramphenicol was added. The flasks were shaken at 200 rpm. The cells were allowed to grow at 37 ° Celsius for approximately 35 hours. The cells were harvested by centrifugation for 5 min at 6000 rpm in an Avanti J-E Beckman Coulter centrifuge. The pellets were resuspended in 20 mM TRIS pH 8.0 and stored at –80 ° Celsius.

Protein Purification

The following day the resuspended pellets were thawed at room temperature and lysed by homogenation. Cell lysate was centrifuged at 12000 rpm for 25 min to separate the bulk of the cell debris. Following lysis, the protein contained in the superantant underwent ammonium sulfate factionation, yet another crude purification step. Ammonium sulfate was gradually dissolved in the supernatant till 45% saturation and then centrifuged at 12,000 rpm for 30 min. A large fraction of containment proteins were removed with this step. Next, more ammonium sulfate was added to the supernatant till the concentration was 90%. The solution was again centrifuged again at 12,000 rpm for 30 min and the supernatant was discarded. The pellet was resuspended in 20 mM TRIS pH 8.0, 2M ammonium sulfate.

Phenyl sepharose

The phenyl sepharose column was equilibrated with 20 mM TRIS pH 8.0, 2M ammonium sulfate. The resuspended pellet was loaded onto the column. Approximately 1L of loading buffer was run over the column. The loading buffer was diluted to 1.6M ammonium sulfate and the column was washed with another 300 ml. The protein was then eluted with 20 mM TRIS pH 8.0, 1M ammonium sulfate. The purity of each fractions was checked according the the Soret/A_{280} using a UV-spectrophotometer. Fractions were pooled and concentrated by 90% ammoniuam sulfate precipitation. The solution was centrifuged at 12,000 rpm for 25 min and the pellet was resuspended in 10 mM potassium phosphate pH 7.0. Ammonium sulfate was then removed by dialysis into 10 mM potassium phosphate pH 7.0.

CM Sepharose Chromatography

The column was equilibrated with 1L of loading buffer, 10 mM potassium phosphate pH 7.0. Afterwards the protein was loaded and washed with approximately 500 ml of loading buffer. The protein was then washed with 200 ml of 10 mM potassium phosphate pH 7.5 and again another 200 ml of 20 mM TRIS pH 8.0. The protein was eluted with 20 mM TRIS pH 8.5. Fractions were pooled and concentrated. Another step of purification was usually needed so fractions were dialysised into 10 mM potassium phosphate pH 7 and another CM column was run. Fractions were run on SDS-PAGE to asses the purity. Pure fractions were pooled and concentrated to 1 ml.

Absorbance Spectroscopy

Absorbance spectra were recorded using a Ocean-Optics UV-vis spectrophotometer (USB 2000). The ferric state of the protein was formed by the addition of potassium ferricyanide followed by desalting on a Sephadex G-25 column in 10mM potassium phosphate, pH 7. The ferrous form of the sample was obtained by adding a slight molar excess of sodium dithionite.

Electrochemistry

Measurements werw carried out using an Ocean-Optics UV-vis spectrophotometer (USB 2000) and an Oakton pH-mV meter (pH 1100 series). A saturated calomel electrode (SCE) was used as a reference in combination with a platinum working electrode. Mid- point potentials (E_{mid}) and reduction potentials (E_{obs}) are reported with reference to a standard hydrogen electrode (SHE). Protein titrations were carried out at 25 °C in argon-saturated 100 mM potassium phosphate buffer, pH 7.0 (5).

Mediators

Redox mediators range: +157 to -440 mV. E_{mid} vs. SHE: 1,2-naphthoquinone (+157 mV), toluylene blue (+115 mV), duroquinone (+5 mV), hexaammineruthenium(III) chloride (+50 mV), pentaaminechlororuthenium(III) chloride (-40 mV), 5,8-dihydroxy-1,4-naphthoquinone (-50 mV), 2,5-dihydroxy-1-4-benzoquinone (-60 mV), 2-hydroxy-1,4-naphthoquinone (-137 mV), anthraquinone-1,5-disulfonic acid (-175 mV), 9,10-anthraquinone-2,6-disulfonic acid (-184 mV), and methyl viologen (-440 mV) (5).

Cell

Final mediator concentration was 25 μM in 100 mM potassium phosphate pH7. To degas the cell, argon was passed through bubblers containing the oxygen scavenging solution and into the cell. The solution was degased for one hour. Protein and sodium dithionite solutions were also degassed. Protein was added to the cell until the soret had reached an absorbance of about 0.5 (5).

Titrations

The sodium dithionite solution was added to the cell in 2 μL increments. The system was allowed to equilibrate for about 5 minutes. E_{obs} was noted for each addition and the corresponding spectra was saved. Addition of sodium dithionite solution continued till there was no further change in absorbance, indicating reduction was complete (5).

Midpoint potentials

Midpoint potential was extracted from the change in absorbance at 424 nm and fitting to equation 3 (5).

X-Ray Crystallography

Before cystallography plates were set up, protein was fully oxidized to its ferric Fe^{3+} form by adding a slight molar excess (a few grains) of potassium ferricyinide to the concentrated 1 ml sample and then shortly vortexing it. Potassium ferricyinide was then removed by loading the protein onto a desalting G-25 sephadex column equilibrated with 10 mM potassium phosphate pH 7.0. The protein was eluted with loading buffer and concentrated to roughly 3

mM and storted at -80 ° C. The final concentration was determined by UV-spectrophotometry.

Protein Crystallization

Crystallization of Parasponia Hb was accomplished by the hanging-drop vapor diffusion technique. The crystalization conditions were 1.6 M ammonium sulfate, 0.1 M MES pH 7.0, 10% (v/v) dioxane and 0.1 M phenol. The well buffer all solutions except for phenol which was added directly to the drop. To form a drop 1.5 μL of protein was mixed with 1.2 μL of well buffer and 0.3 μL of 0.1 M phenol was then added. Single crystals appeared in less than 24 hours at room temperature.

Structure Solution

The diffraction data were collected on a Rigaku/MSC home source generator at 120 K and processed using d*TREK. The CCP4 program suites was used to solve the structure by molecular replacement with the wild-type rice Hb (PDB code 1BIN). Both hexacoordinate and pentacoordinate Hb models were tested as possible molecular replacement models. In short, Rice Hb proved to be the best bet as a molecular replacement model for having produced the lowest initial crystallographic R-value of ~0.45. O software was used to manually manipulate and rebuild the structure.

REFERENCES

1. Dordas C., Rivoal J., & Hill R. Plant Hemoglobins, Nitric Oxide, and Hypoxic Stress. *Annal of Bot,* Vol. 91, 173-178 (2003).
2. Franche C., Diouf D., Laplaze L., Auguy F., Frutz T., Rio M., Dyhoux E., & Bogusz D. Soyebean (lbc3), Parasponia, and Trema Hemoglobin Gene Promoters Retain Symbiotic and Nonsymbiotic Specificity in Transgenic Casuarinaceae: Implications for Hemoglobin Gene Evolution and Rook Nodule Symbioses. *MPMI.* Vol. 11, 887-894 (1998).
3. Garrocho-Villegas V, Gopalasubramaniam SK, Arredondo-Peter R. Plant hemoglobins: What we know six decades after their discovery. [Epub ahead of print]
4. Goodman M. D. and Hargrove M. S. Quaternary Structure of Rice Nonsymbiotic Hemoglobin. *JBC*. Vol. 276, 6834-39 (2001).
5. Halder P., Trent J. T. III & Hargrove M. S. Influence of the Protein Matrix on Intramolecular Histidine Ligation in Ferric and Ferrous Hexacoordinate Hemoglobins. *Proteins*. Vol. 66, 172-82 (2007).
6. Hargrove, M. S. A Flash Photolysis Method to Characterize Hexacoordinate Hemoglobin Kinetics. *Biophys. J*., Vol. 79, 631-51 (2000A).
7. Hargrove M. S., Brucker E. A., Stec B., Sarath G., Arredondo-Peter R., Klucas R. V., Olson J. S. and Phillips G. N. Jr. Crystal Structure of a Nonsymbiotic Plant Hemoglobin. *Structure*. Vol. 8, 1005-14 (2000B).

8. Kundu S., Trent J. T. III, & Hagrove M. S. Plants, Humans and Hemoglobins. *Trends Plant Sci.* Vol. 8, 387-93 (2003A).

9. Marmo Moreira L, Lima Poli A, Costa-Filho AJ, Imasato H. Pentacoordinate and hexacoordinate ferric hemes in acid medium: EPR, UV-Vis and CD studies of the giant extracellular hemoglobin of Glossoscolex paulistus. *Biophys Chem,* Vol. 124, 62-72 (2006).

10. McPherson, Alexander. Introduction to Macromolecular Crystallography. John Wiley & Sons, Inc., New Jersey. 2003.

11. Smagghe B. J., Suman K., Hoy J. A., Halder P., Weiland T. R., Savage A., Venugopal A., Goodman M., Premer S., & Hargrove M. S. Role of Phenylalanine B10 in Plan Nonsymbiotic Hemoglobins. *Biochemistry*, Vol. 45, 9735-45 (2006B).

12. Trinick MJ, Goodchild DJ, Miller C. Localization of Bacteria and Hemoglobin in Root Nodules of Parasponia andersonii Containing Both Bradyrhizobium Strains and Rhizobium leguminosarum biovar trifolii. *Environ Microbiol,* Vol.55, 2046-2055.

13. Trent JT 3rd, Kundu S, Hoy JA, Hargrove MS. Crystallographic analysis of synechocystis cyanoglobin reveals the structural changes accompanying ligand binding in a hexacoordinate hemoglobin. *J Mol Biol,* Vol. 3411097-108 (2004).

14. Trent J. T. III and Hargrove M. S. A Ubiquitously Expressed Human Hexacoordinate Hemoglobin. *JBC*. Vol. 277, 19538-45 (2002).

15. Wittenberg JB, Wittenberg BA, Gibson QH, Trinick MJ, Appleby CA. The kinetics of the reactions of Parasponia andersonii hemoglobin with oxygen, carbon monoxide, and nitric oxide. *J Biol Chem,* Vol. 261, 13624-31 (1986).